



## UvA-DARE (Digital Academic Repository)

### Heparan sulfate proteoglycans: key moderators of the interaction of multiple myeloma with the bone marrow niche

Ren, Z.

**Publication date**

2019

**Document Version**

Other version

**License**

Other

[Link to publication](#)

**Citation for published version (APA):**

Ren, Z. (2019). *Heparan sulfate proteoglycans: key moderators of the interaction of multiple myeloma with the bone marrow niche*. [Thesis, fully internal, Universiteit van Amsterdam].

**General rights**

It is not permitted to download or to forward/distribute the text or part of it without the consent of the author(s) and/or copyright holder(s), other than for strictly personal, individual use, unless the work is under an open content license (like Creative Commons).

**Disclaimer/Complaints regulations**

If you believe that digital publication of certain material infringes any of your rights or (privacy) interests, please let the Library know, stating your reasons. In case of a legitimate complaint, the Library will make the material inaccessible and/or remove it from the website. Please Ask the Library: <https://uba.uva.nl/en/contact>, or a letter to: Library of the University of Amsterdam, Secretariat, P.O. Box 19185, 1000 GD Amsterdam, The Netherlands. You will be contacted as soon as possible.

CHAPTER

# 3

## **Syndecan-1 promotes Wnt/ $\beta$ -catenin signaling in Multiple Myeloma by presenting Wnts and R-spondins**

Zemin Ren<sup>1,2,3</sup>, Harmen van Andel<sup>1,2,3</sup>, Wim de Lau<sup>4</sup>, Robin B. Hartholt<sup>5</sup>, Madelon M. Maurice<sup>6</sup>, Hans Clevers<sup>4</sup>, Marie José Kersten<sup>2,7</sup>, Marcel Spaargaren<sup>1,2,3,8</sup>, Steven T. Pals<sup>1,2,3,8</sup>

<sup>1</sup>Department of Pathology, Academic Medical Center, University of Amsterdam, The Netherlands;

<sup>2</sup>Lymphoma and Myeloma Center Amsterdam – LYMMCARE, The Netherlands; <sup>3</sup>Cancer Center Amsterdam (CCA), Amsterdam, The Netherlands; <sup>4</sup>Hubrecht Institute, University Medical Center Utrecht, and Princess Maxima Center, Utrecht, The Netherlands; <sup>5</sup>Department of Plasma Proteins, Sanquin-AMC Landsteiner Laboratory, Amsterdam, the Netherlands; <sup>6</sup>Department of Cell Biology, University Medical Center Utrecht, Utrecht, the Netherlands; <sup>7</sup>Department of Hematology, Academic Medical Center, University of Amsterdam, The Netherlands.

<sup>8</sup>The authors share last authorship

**Blood (2018) 131(9):982-994**

## Abstract

Multiple myeloma (MM) is characterized by the expansion of malignant plasma cells in the bone marrow (BM). Most MMs display aberrant Wnt/ $\beta$ -catenin signaling, which drives proliferation; however, they lack oncogenic Wnt-pathway mutations, suggesting activation by autocrine Wnt ligands and/or paracrine Wnts from the BM microenvironment. Expression of the heparan sulfate proteoglycan (HSPG) syndecan-1 is a hallmark of MM. Syndecan-1 is a critical player in the complex reciprocal interaction between MM cells and their BM niche, mediating growth factor/cytokine binding and signaling by its heparan sulfate (HS) chains. Here, by means of CRISPR/Cas9-mediated knockout and doxycycline-inducible shRNA-mediated knockdown of EXT1, a critical enzyme for HS polymerization, we demonstrate that the HS-chains decorating syndecan-1 mediate aberrant Wnt-pathway activation in MM. HS-deficient MM cells exhibited a strongly decreased autocrine Wnt/ $\beta$ -catenin pathway activity and a reduced Wnt-pathway-dependent proliferation. In addition, we demonstrate that Wnts bind to the HS side-chains of syndecan-1 and that this binding contributes to paracrine Wnt-pathway activation through the Wnt-receptor Frizzled. Furthermore, in a HS-dependent fashion, syndecan-1 also binds osteoblast-produced R-spondin, which represses Frizzled degradation by activation of LGR4, an R-spondin receptor aberrantly expressed on MM cells. Co-stimulation with R-spondin, and its binding to HS chains decorating syndecan-1, are indispensable for optimal stimulation of Wnt-signaling in MM. Taken together, our results identify syndecan-1 as a crucial component of the Wnt-signalosome in MM cells, binding Wnts and R-spondins to promote aberrant Wnt/ $\beta$ -catenin signaling and cell growth, and suggest HS and its biosynthetic enzymes as potential targets for the treatment of MM.

## Introduction

Multiple myeloma (MM) is an in most patients incurable hematologic neoplasm characterized by the accumulation of malignant plasma cells in the bone marrow (BM). Notwithstanding the diversity of underlying structural and numerical genomic abnormalities,<sup>1-3</sup> virtually all MMs are highly dependent on a protective BM microenvironment for growth and survival.<sup>4</sup> The membrane-bound heparan sulfate proteoglycan (HSPG) syndecan-1 has been identified as a critical player in this complex reciprocal interaction between MM cells and their BM 'niche'.<sup>5,6</sup> Consequently, targeting syndecan-1 could be employed as strategy to disconnect MM cells from their BM 'niche'.

Expression of the HSPG syndecan-1 is characteristic of plasma cells and their malignant MM counterparts<sup>7</sup> and plays a crucial role in MM cell growth and survival.<sup>6,8,9</sup> HSPGs are a class of extracellular matrix or cell-membrane-bound glycoproteins designed to specifically bind and regulate the bioactivity of soluble protein ligands<sup>10,11</sup> and play an essential role in the spatial control of extracellular signals regulating cell growth, survival, and differentiation, including tumorigenesis.<sup>11-13</sup> They consist of a protein core with covalently attached polysaccharide heparan sulfate (HS) chains. These HS chains undergo a series of processing reactions involving *N*-deacetylation/*N*-sulfation, epimerization, and *O*-sulfation.<sup>10,11</sup> This endows HS chains with highly modified domains, which provide specific docking sites for a large number of bioactive molecules, such as growth factors and cytokines, and serve a variety of functions ranging from immobilization and concentration to distinct modulation of signaling.<sup>13-15</sup> On MM cells, syndecan-1 is the principal, if not sole, HSPG.<sup>8,9</sup> The HS-chains decorating syndecan-1, mediate interaction between the tumor cells and growth factors from the BM microenvironment,<sup>6</sup> including hepatocyte growth factor (HGF), epidermal growth factor (EGF)-family members, and APRIL.<sup>5,8,16</sup> In addition, syndecan-1 may also regulate Wnt signaling,<sup>17</sup> which has been implicated in driving MM proliferation and is associated with disease progression, dissemination, and drug resistance.<sup>18-22</sup>

Wnts are lipid-modified glycoproteins that function as typical niche factors since they are relatively unstable and insoluble due to their hydrophobic nature, which constrains long-range signalling.<sup>23</sup> Binding of a Wnt ligand to its receptor Frizzled (Fzd) initiates a signaling cascade that ultimately results in stabilization and nuclear translocation of the Wnt effector  $\beta$ -catenin. In cooperation with TCF/LEF family transcription factors this orchestrates a transcriptional program<sup>24,25</sup> including c-Myc and Cyclin D1 which play crucial roles in the pathogenesis of MM.<sup>26-28</sup> The turnover of the Wnt receptor Fzd is critically regulated by LGR-family receptors and their cognate R-spondin ligands. R-spondin/LGR binding alleviates the inhibitory effect of two homologous membrane-bound E3 ubiquitin-ligases, ZNRF3 and RNF43, which promote Fzd internalization, thereby controlling the amplitude of Wnt signaling.<sup>29-32</sup>

Aberrant Wnt signaling in cancer typically results from mutations in *APC*,  $\beta$ -catenin (*CTNNB1*), or *AXIN* that drive constitutive, ligand-independent pathway activation.<sup>32</sup> However, MMs displaying active Wnt signaling do not harbor these classic mutations. Instead oncogenic Wnt pathway activity in MM involves autocrine and/or paracrine Wnt ligands,<sup>19,21,32,33</sup> and is potentiated by aberrant expression and turnover of Wnt (co-)receptors and transcriptional activators, as well as by loss of negative Wnt pathway regulators. These activating events include aberrant expression of the R-spondin receptor *LGR4*,<sup>34</sup> and of the transcriptional co-activator *BCL9*,<sup>35,36</sup> epigenetic silencing of the feed-back inhibitors sFRPs and *DKK1*,<sup>21,33</sup> and mutational inactivation of *CYLD*, a deubiquinating enzyme that negatively regulates Wnt.<sup>37</sup> Given the ligand-dependence of Wnt pathway activation in MM, targeting of Wnt (co)receptors, disconnecting the MM cells from their growth-promoting microenvironment, is a potentially promising therapeutic strategy for MM. This prompted us to explore the specific contribution of syndecan-1 HS to Wnt-signaling activation in MM.

## Materials and Methods

### Cell culture and treatment

The human multiple myeloma cell lines (HMCLs) LME-1, LP1, OPM-2, RPMI 8226 (RPMI), XG-1, RIES and XG-3 were cultured in IMDM medium (Invitrogen Life Technologies) containing 10% FBS (Invitrogen Life Technologies), 100 units/ml penicillin (Sigma Aldrich), 100 µg/ml streptomycin (Sigma Aldrich). For XG-1, XG-3, LME-1 and RIES, medium was supplemented with 500 pg/mL IL-6 (Prospec). Primary MM cell samples were derived from patients diagnosed at the Academic Medical Center, Amsterdam, the Netherlands. This study was conducted and approved by the AMC Medical Committee on Human Experimentation. Informed consent was obtained in accordance with the Declaration of Helsinki. For signal transduction experiments, recombinant hWnt3a (R&D systems) was used at 100ng/mL, recombinant hR-spondin1 at 50ng/mL (R&D systems) unless otherwise stated. Wnt inhibitors used were IWP-2 (2.5uM, Stemgent) and LGK974 (2.5uM, StemRD). For heparitinase treatment, 300,000 MM cells were treated with 5 mU heparitinase (Amsbio) for 60 min at 37°C.

### Cloning, transfection and transduction

The dnTCF4 construct were obtained from addgene (52961); S33Y β-catenin was generated by inserting S33Y β-catenin into the HPAI site of pHIV-H2BmRFP (Addgene 18982). pTRIPZ-sh*EXT1* was customly constructed. In short, a 97-mer template was inserted in the XhoI/EcoRI site of the pTRIPZ vector (Thermo Scientific, Waltham, MA). The targeting sequences was GCACATATCACGTAACAGT. pLentiCrispr-sg*EXT1* was constructed by inserting sg*EXT1* (GACCCAAGCCTGCGACCACG, chr8:118849372-118849391; GTCTGGTTCCTCGTGGTCGC, chr8:118849383-118849402) in pLentiCrispr (addgene 52961) as previously described.<sup>38</sup> TOP-GFP.mCh and FOP-GFP.mCh (Addgene 35491 and 35492) were kind gifts by David Horst.<sup>39</sup> c-Myc construct were obtained from Addgene (18770). Mutant R-spondin-ΔTSP was constructed by inserting R-spondin1 lacking TSP domain and C-terminal basic amino-acid-rich domain into pcDNA3. The control R-spondin-ΔAA is constructed by inserting R-spondin1 lacking C-terminal basic amino-acid-rich domain into pcDNA3. Lentiviral transduction was performed as described before,<sup>34</sup> For retroviral transduction, constructs were transfected into Phoenix-GALV cells with genius DNA transfection reagent (Westburg). MM cells were spininfected for 60 minutes at 1800 RPM at 33 °C in RetroNectin-coated plates. Transduced cells were sorted by flow cytometry.

### In vitro cell growth and apoptosis

In vitro cell growth and apoptosis were performed as described before.<sup>6</sup> For full detail, see Supplemental methods.

### **Confocal microscopy**

The reduction in heparan sulfate expression after *EXT-1* knock-out was evaluated by confocal microscopy. For full detail, see Supplemental methods.

### **Cell cycle analysis**

Cells were incubated for 1h with 20 $\mu$ M BrdU (Sigma Aldrich) and subsequently fixed in ice-cold 70% ethanol. Cells were washed twice with PBS/0.1%BSA and incubated with 0.4mg/ml pepsin/0.2mM HCL for 30 minutes on RT, spun down and subsequently incubated in 2M HCL for 25 minutes at 37°C. Then cells were washed with 0.05% Tween-20/0.5%BSA in PBS and stained for 30 minutes with anti-BrdU FITC (clone B44, BD). After washing, cells were stained with 0.1 $\mu$ M TO-PRO-3-Iodide (Invitrogen Life Technologies) in PBS/0.5% BSA containing 500 $\mu$ g/ml RNase-A (Bioke, Leiden, The Netherlands) for 15 minutes at 37°C. Cell cycle distribution was analyzed by flow cytometry.

For cell cycle analysis of Wnt responsive cells (Fig. S4), see Supplemental methods.

### **Immunoblotting**

Immunoblotting were perform as describe before.<sup>34</sup> For full detail, see Supplemental methods.

### **Flow cytometry**

Cell staining was analyzed by flow cytometry. For full detail, see Supplemental methods.

## **Results**

### **Human myeloma cell lines display constitutive Wnt-signaling.**

Previous studies have shown that activation of the canonical Wnt pathway is common in advanced primary MMs and in human myeloma cell lines (HMCLs).<sup>19-22</sup> This aberrant Wnt signaling activity is driven by autocrine and/or paracrine Wnt ligands and promotes MM proliferation.<sup>19,22</sup> To confirm and extend these findings, we expressed a dominant negative TCF4 (dnTCF4) from a lentiviral vector containing a mCherry marker in HMCLs and measured the percentage of transduced cells over time. dnTCF4 transduced myeloma cells were rapidly outcompeted, whereas the percentage of control vector transduced cells was stable (Fig.1A and S1A), confirming that growth of these HMCLs indeed depends on Wnt signaling.

To explore the possible involvement of autocrine Wnt ligands, we tested the effect of the Wnt secretion inhibitors IWP-2 and LGK974 on myeloma growth. These small molecules inhibit the activity of Porcupine, a membrane-bound acyltransferase that is essential for the secretion of Wnt proteins.<sup>40,41</sup> We found that both inhibitors significantly inhibit the

growth of LP1 and LME1 (Fig.1B) and that they indeed inhibit autocrine Wnt signaling (Fig. S1B). Despite the significant reduction in cell numbers, both inhibitors hardly affected cell viability (Fig.S1C). Importantly, downstream activation of Wnt signaling by an active mutant  $\beta$ -catenin (S33Y  $\beta$ -catenin) overcame the growth inhibition by IWP2 and LGK974 (Fig.1C). Taken together, these findings suggest that autocrine Wnt ligands are involved in Wnt pathway activation and cell growth in these HMCLs.

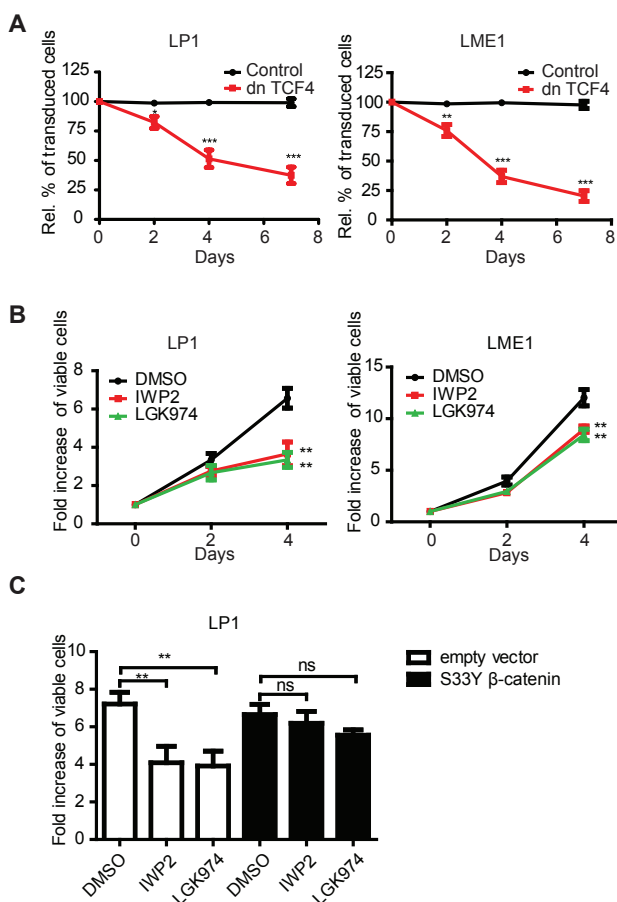


**Figure 1. HMCLs display constitutive Wnts signaling.** (A) Percentage of transduced cells in HMCLs transduced with empty vector control or dn.TCF4 expressed from bicentric lentiviral vectors, relative to day 0. The mean  $\pm$ SD of 3 independent experiments in triplicate is shown. \*,  $P \leq 0.05$ ; \*\*,  $P \leq 0.01$ ; \*\*\*,  $P \leq 0.001$  using unpaired student's t-test. (B) Flow cytometry analysis of the effect of small molecule Wnt secretion inhibitor IWP-2 (2.5 $\mu$ M) and LGK974 (2.5 $\mu$ M) on HMCLs cell expansion in a 4 days' time course, relative to day 0. The mean  $\pm$ SD of 3 independent experiments in triplicate is shown. \*\*,  $P \leq 0.01$  using unpaired student's t-test. (C) Flow cytometry analysis of the effect of small molecule Wnt secretion inhibitor IWP-2 (2.5 $\mu$ M) and LGK974 (2.5 $\mu$ M) on the expansion of HMCL LP1 transduced with S33Y mutant  $\beta$ -catenin or the empty vector control in a 4 days' time course, relative to day 0. The mean  $\pm$ SD of 3 independent experiments in triplicate is shown. ns,  $P > 0.05$ ; \*\*,  $P \leq 0.01$  using one-way ANOVA with Bonferroni correction.

### **Deletion of heparan sulfate by *EXT1* knock-out inhibits Wnt-signaling in HMCLs**

HSPGs, including syndecan-1, have previously been implicated in the regulation of Wnt signaling, including Wnt-mediated tumorigenesis.<sup>17</sup> To explore the possible involvement of syndecan-1 HS in Wnt signaling in MM, we deleted the HS co-polymerase *EXT1* in HMCLs by CRISPR/Cas9-mediated knock-out (ko). This completely abolished cell-surface HS expression (Fig. 2A). To determine its effect on Wnt signaling, we measured the levels of nuclear and cytoplasmic  $\beta$ -catenin (Fig. 2B), a key component of canonical Wnt signaling. In addition, TCF4-mediated Wnt-reporter activity was assessed in LP1 cells stably transduced with a fluorescent Wnt-reporter (TOP-GFP) and co-expressing a histone2B (H2B)/mCherry fusion protein as transduction-marker. As control, LP1 cells were transduced with FOP-GFP (Fig.2C). As shown in Fig.2B, ko of *EXT1* resulted in reduced  $\beta$ -catenin levels in both the nucleus and cytoplasm in three HMCLs studied. In contrast, phosphorylation of AKT and the MAP kinases ERK1/2, typically reflecting activation of growth factor signaling, was not affected in LME1 and LP1(Fig.S2). Furthermore, deletion of *EXT1* resulted in a strong reduction in the percentage of TOP-GFP positive cells in LP1 (Fig.2D). We also determined the effect of *EXT1* ko on the expression of the Wnt target genes *c-Myc* and *CCND1* (*Cyclin D1*).<sup>20</sup> As shown in Fig.2E, *EXT1* ko resulted in reduced expression of c-Myc and Cyclin-D1. Taken together, these data show that loss of HS leads to reduced baseline Wnt pathway activity in HMCLs, suggesting that HSPGs mediate Wnt signaling in MM.

### **Loss of HS inhibits MM cell growth by attenuating Wnt signaling.**

We have previously shown that knockdown (kd) of either *EXT1* or *syndecan-1* inhibits the growth of MM cells both *in vitro* and *in vivo*.<sup>6</sup> To confirm and extend these findings, we performed *EXT1* kd in a panel of HMCLs (Fig.S3A). Loss of HS resulted in a significant inhibition of cell growth in 4 out of 6 HMCLs (Fig.3A and S3C). Importantly, similar results were also obtained in primary MM cells. Since the poor *ex vivo* viability and growth of these cells prohibited viral transduction and subsequent selection to (inducible) silence *EXT1* by shRNA, we employed heparitinase to remove HS. This resulted in a complete depletion of HS chains from the MM cell surface (Fig.3B), resulting in a significant growth inhibition (Fig.3C).

*EXT1* kd only weakly affected cell viability in 2 of the HMCLs and did not induce apoptosis (Fig.S3D and Fig.3D); however, it strongly decreased the percentage of cells in S-phase and slightly increased the percentage of cells in the sub-G1 phase, as determined by measuring DNA content and BrdU incorporation (Fig.3E). Similarly, removal of HS in primary MM by heparitinase did not induce significant cell death (Fig.S3E). These data indicate that loss of HS mainly affects MM growth by attenuating proliferation. Importantly, this growth inhibition could not be overcome by co-culture of MM cells with bone marrow stromal cells (BMSCs) (Fig.3F).

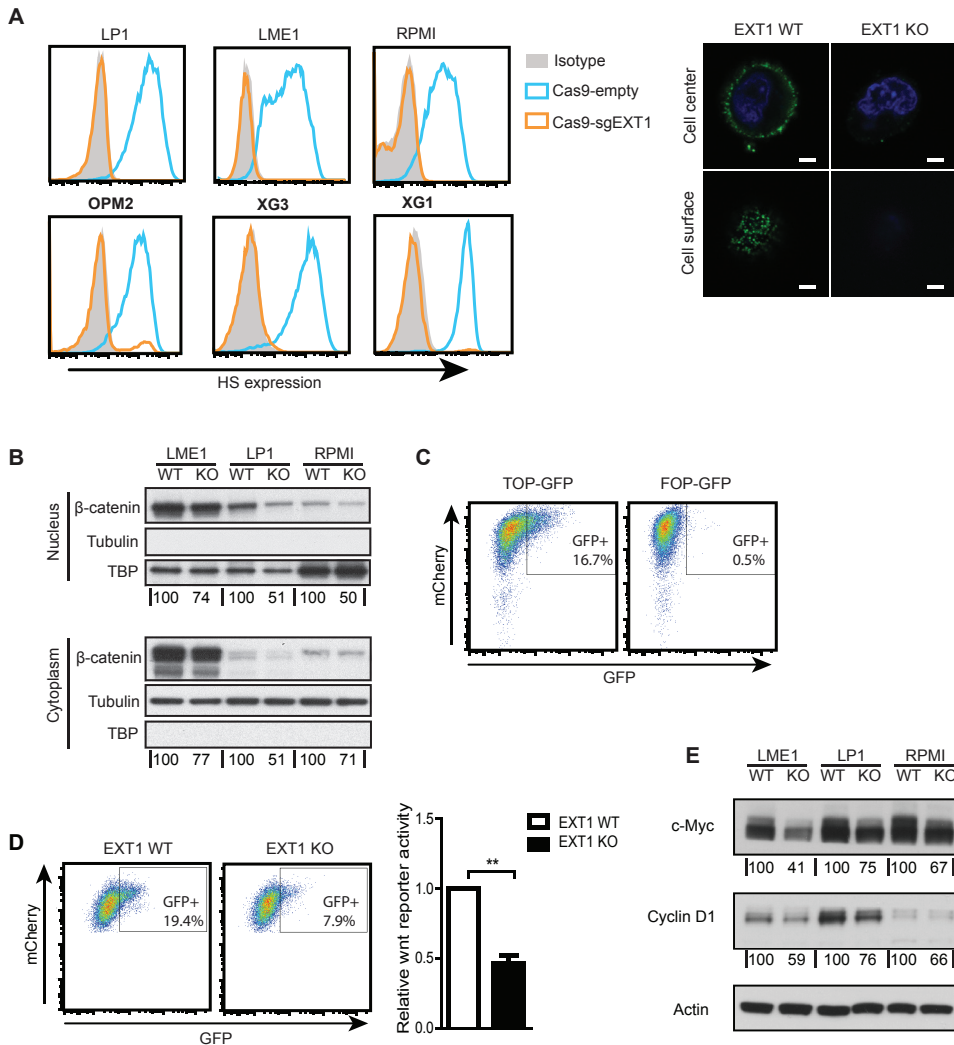


**Figure 2. Deletion of heparan sulfate by EXT1 knock-out reduces Wnt-signaling in HMCLs.** (A) Upper panel: Flow cytometry analysis of cell surface expression of HS in control transduced cells (Cas9-empty control) or upon CRISPR/CAS9-mediated EXT1 KO (Cas9-sgEXT1) in HMCLs; Lower panel: Confocal microscopy analysis of HS expression in control transduced cells (EXT1 WT) or upon CRISPR/CAS9-mediated EXT1 knock out (EXT1 KO) in HMCL LME1. Scale bars represent 2.5  $\mu$ m. (B) Analysis of the nuclear and cytoplasmic distribution of  $\beta$ -catenin in HMCLs after EXT1 KO by western blot. Tubulin (cytoplasm) and TBP (nucleus) served as a fractionation and loading controls. For quantification, the expression level in WT cells was normalized to an arbitrary level of 100 units (C) Flow cytometry analysis of Wnt reporter activity in LP1 cells transduced with Wnt-signaling reporter TOP-GFP or control FOP-GFP. (D) Flow cytometry analysis of Wnt reporter activity in EXT1 WT or EXT1 KO LP1 cells. A representative plot is shown in left. Quantification of Wnt reporter activity is plotted as the percentage of mCherry/GFP double positive live cells (right). The mean  $\pm$ SD of 3 independent experiments in triplicate is shown. \*\*,  $P \leq 0.01$  using one sample t-test. (E) Analysis of c-Myc and Cyclin D1 expression after EXT1 KO by western blot. Actin served as loading controls. For quantification, the expression level in WT cells was normalized to an arbitrary level of 100 units.

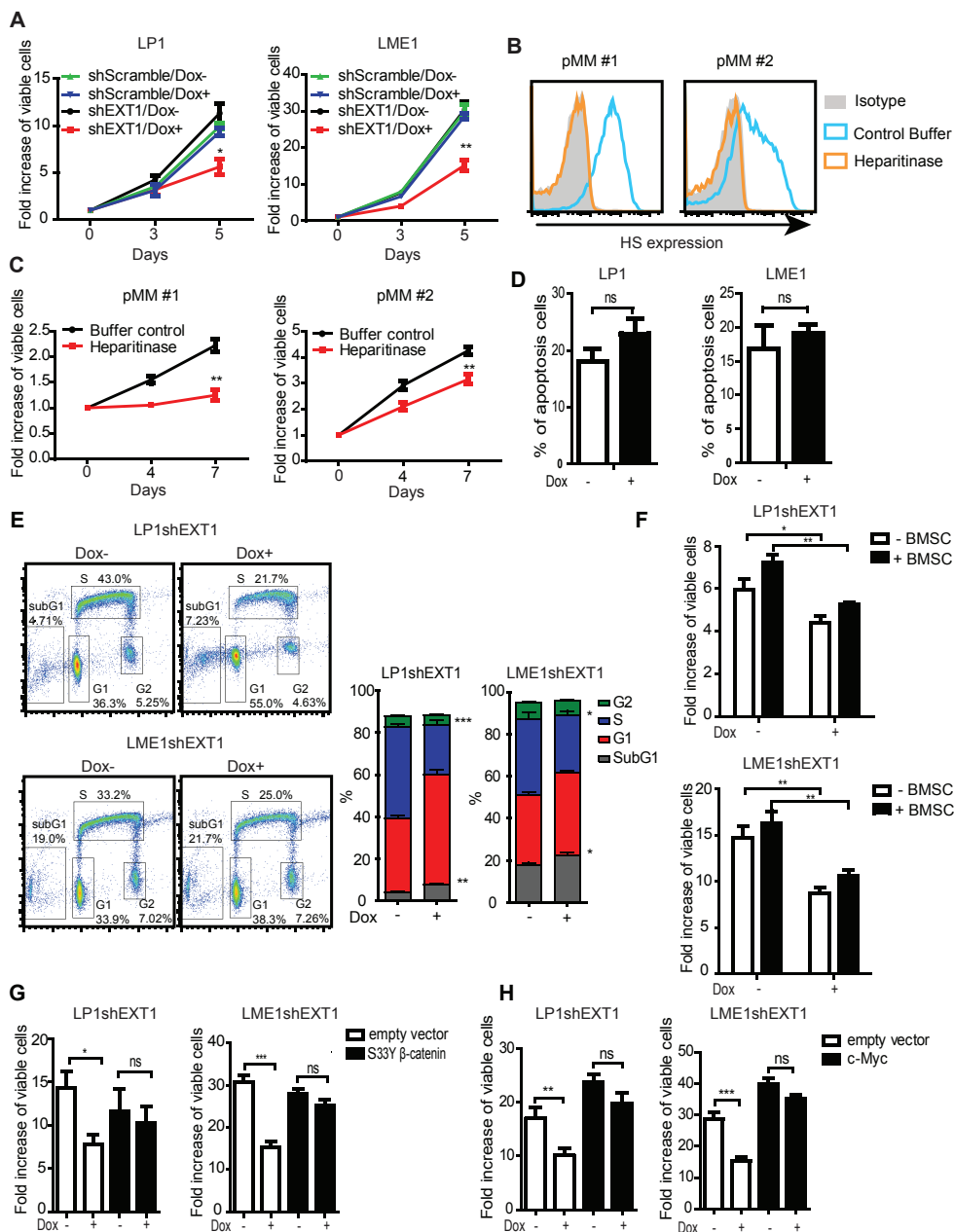


**Figure 3. Loss of HS inhibits MM cell growth by attenuating Wnt signaling.** (A) Flow cytometry analysis of the effect of doxycycline (Dox)-induced EXT1 knock down (kd) on MM cell expansion at 5 days culture, relative to day 0. shScramble is used as control. The mean  $\pm$ SD of 3 independent experiments in triplicate is shown, \*,  $P \leq 0.05$ ; \*\*,  $P \leq 0.01$  using unpaired student's t-test. (B) Flow cytometry analysis of primary MM cell surface HS expression after heparitinase treatment. (C) Flow cytometry analysis of primary MM cell expansion after heparitinase or control buffer treatment. A representative plot for 2 independent experiments is shown. \*\*,  $P \leq 0.01$  using unpaired

student's t-test. (D) Flow cytometry analysis of the effect of doxycycline (Dox)-induced *EXT1* knock down (kd) on HMCLs apoptosis. The mean  $\pm$ SD of 3 independent experiments in triplicate is shown, ns (not significant), using unpaired student's t-test. (E) Left: representative plot of cell cycle analysis after BrdU incorporation upon doxycycline (Dox) induced *EXT1* kd in HMCLs. Right: quantification of cell cycle distribution after BrdU incorporation in doxycycline-induced *EXT1* kd in HMCLs, The mean  $\pm$ SD of 3 independent experiments in triplicate is shown. \*,  $P \leq 0.05$ ; \*\*,  $P \leq 0.01$ ; \*\*\*,  $P \leq 0.001$  using unpaired student's t-test. (F) Flow cytometry analysis of the effect of doxycycline (Dox)-induced *EXT1* kd on the expansion of HMCLs in the presence of BMSC in 4 days. The mean  $\pm$ SD of 3 independent experiments each performed in triplicate is shown. \*,  $P \leq 0.05$ ; \*\*,  $P \leq 0.01$  using one-way ANOVA with Bonferroni correction. (G) Flow cytometry analysis of the effect of doxycycline (Dox)-induced *EXT1* kd on the expansion of HMCLs transduced with S33Y  $\beta$ -catenin or empty control vector in 5 days. The mean  $\pm$ SD of 3 independent experiments in triplicate is shown. ns,  $P > 0.05$ ; \*,  $P \leq 0.05$ ; \*\*\*,  $P \leq 0.001$  using one-way ANOVA with Bonferroni correction. (H) Flow cytometry analysis of the effect of doxycycline (Dox)-induced *EXT1* kd on the expansion of HMCLs transduced with c-Myc or empty control vector in 5 days. The mean  $\pm$ SD of 3 independent experiments in triplicate is shown. ns,  $P > 0.05$ ; \*\*,  $P \leq 0.01$ ; \*\*\*,  $P \leq 0.001$ , using one-way ANOVA with Bonferroni correction.

We next studied whether the growth inhibition by *EXT1* kd was causally related to inhibition of Wnt signaling. To this end, we transduced LP1 and LME1 cells with the active mutant  $\beta$ -catenin (S33Y  $\beta$ -catenin), which activates Wnt signaling in the absence of ligand. Interestingly, *EXT1* kd did not cause growth inhibition in mutant  $\beta$ -catenin (S33Y  $\beta$ -catenin) transduced cells while *EXT1* kd in empty vector transduced cells resulted in a strong growth reduction (Fig.3G). These findings suggest that the growth reduction by loss of HS is largely due to Wnt signaling inhibition. In view of our observation that *EXT1* ko markedly reduces the expression of Wnt target c-Myc (Figure 2E), an established key player in B-cell<sup>42</sup> and MM<sup>43</sup> cell proliferation, we explored the possible role of c-Myc in the observed *EXT1* kd mediated growth reduction. To this end, we overexpressed c-Myc in LP1 and LME1 cells (Fig.S3F). In line with a previous study,<sup>43</sup> this enhanced MM cell growth. *EXT1* kd in empty vector transduced LP1 and LME1 cells resulted in a strong growth reduction (Fig.3H). However, in c-Myc overexpressing cells, it did not significantly inhibit growth (Fig.3H), suggesting that c-Myc downregulation plays an important role in the growth inhibition observed upon HS loss.

### Loss of HS impairs Wnt pathway activation by paracrine Wnts.

Although Wnt pathway is aberrantly activated in MM cells, these cells can still respond to exogenous Wnt ligands.<sup>19</sup> Within the BM microenvironment, stromal cells secrete Wnt ligands,<sup>19,22,44,45</sup> whereas (pre)osteoblasts produce R-spondins, which can strongly potentiate Wnt signaling in MM cells.<sup>34</sup> To model the response of MM cells to paracrine Wnts and/or R-spondins, we stimulated a panel of 6 HMCLs, containing the TOP-GFP Wnt reporter, with either Wnt3a, R-spondin, or Wnt3a plus R-spondin. As shown in Fig. 4A, the HMCLs showed a heterogeneous response to these stimuli. Stimulation of OPM2 and XG3 with Wnt3a alone induced strong Wnt reporter activity. In LME1, XG1 and RIES, stimulation with Wnt3a alone resulted in a minimal response, but the combination of Wnt3a and R-spondin led to a huge increase of the reporter activity. In line with our results presented in Fig.1 and Fig. 2, LP1 cells displayed a high basal Wnt reporter activity as a consequence of high autocrine Wnt signaling, and therefore showed a moderate response to Wnt3a and R-spondin stimulation (Fig. 4A, S6 and S7).

To assess whether the HS chains decorating syndecan-1 play a role in Wnt pathway activation by exogenous/paracrine Wnts, we employed OPM2 and XG3, the HMCLs with a high Wnt3a response that is largely independent of co-stimulation via R-spondin/LGR4. As shown in Fig.4B, Wnt3a stimulation resulted in cytoplasmic and nuclear accumulation of  $\beta$ -catenin, which were clearly inhibited in *EXT1* ko cells. Also, Wnt3a-induced reporter activity in the *EXT1* ko cells was strongly diminished compared to empty vector transduced control cells (Fig.4C). Interestingly, in line with previous studies,<sup>46,47</sup> the Wnt-responsive

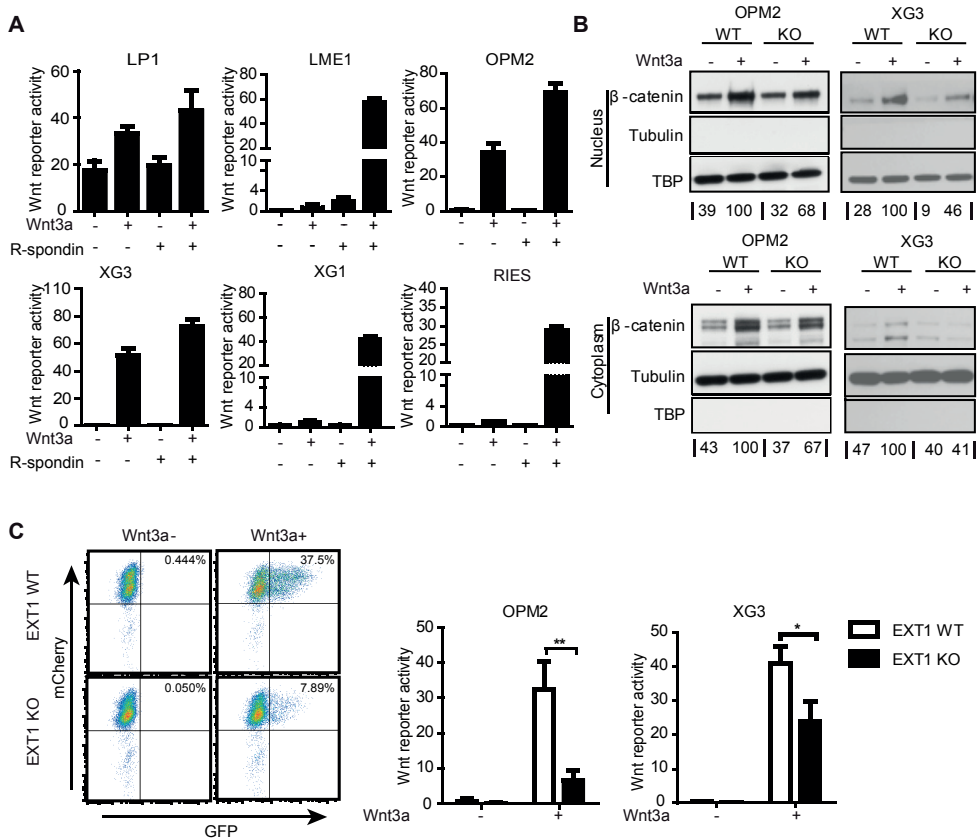


**Figure 4. Loss of HS impairs Wnt pathway activation by paracrine Wnts.** (A) Flow cytometry analysis of Wnt reporter activity in 6 TOP-GFP-transduced HMCLs treated with Wnt3a, R-spondin or both. Wnt reporter activity is plotted as the percentage of mCherry/TOP.GFP double positive cells. The mean  $\pm$ SD of 3 independent experiments in triplicate is shown. (B) Western blot analysis of the nuclear and cytoplasmic distribution of  $\beta$ -catenin in control transduced (WT) or *EXT1* knock out (KO) HMCLs after treatment with Wnt3a. Tubulin (cytoplasm) and TBP (nucleus) served as fractionation and loading controls. For quantification, the expression level in Wnt3a treated WT cells was normalized to an arbitrary level of 100 units. (C) Flow cytometry analysis of Wnt reporter activity in control transduced (*EXT1* WT) or *EXT1* KO HMCLs after treatment with Wnt3a. Left panel: representative picture of TOP-GFP reporter assay in HMCL OPM2 is shown. Right panel: Wnt reporter activity is plotted as the percentage of mCherry/TOP.GFP double positive cells. The mean  $\pm$ SD of 3 independent experiments in triplicate is shown. \*,  $P \leq 0.05$ ; \*\*,  $P \leq 0.01$  using one-way ANOVA with Bonferroni correction.

subpopulation of cells is enriched for cells in the G2/M-phase of the cell cycle (Fig.S4). Furthermore, enzymatic removal of cell-surface HS by heparitinase similarly attenuated Wnt/ $\beta$ -catenin signaling (Fig.S5). Taken together, these results demonstrate that HS plays an important role in Wnt3a-induced Wnt pathway activation.

### **Loss of HS mitigates the potentiating effect of R-spondin on Wnt signaling.**

Recently, R-spondin family proteins have emerged as important positive regulators of Wnt signaling.<sup>29,30</sup> Within the MM bone-marrow niche, R-spondins are abundantly expressed by (pre)osteoblast.<sup>101</sup> To study the role of HS in Wnt pathway activation by exogenous R-spondins, we employed the HMCLs XG1, LME1 and RIES which require co-stimulation via R-spondin/LGR4 for substantial Wnt pathway activation (Fig.4A). Wnt signaling was assessed by measuring accumulation and nuclear translocation of  $\beta$ -catenin, and by quantifying TCF4-mediated Wnt-reporter activity. As is shown in Fig.5A, simultaneous stimulation with R-spondin and Wnt3a resulted in a robust  $\beta$ -catenin stabilization and nuclear translocation. These responses were dramatically impaired in *EXT1* ko cells. In line with these findings, removal of HS from primary MM cells by heparitinase strongly attenuated Wnt3a and R-spondin induced  $\beta$ -catenin accumulation (Fig.5B). *EXT1* ko also significantly impeded Wnt reporter activation (Fig.5C and S6). Taken together, these results demonstrate that HS play a crucial role in Wnt3a and R-spondin induced Wnt pathway activation.

3

### **Loss of HS interferes with upstream, receptor proximal, Wnt-signaling.**

Previous studies have shown that HSPG localization and function are not restricted solely to the cell surface. Specifically, HSPGs localized in the nucleus have been implicated in the regulation of transcription factor binding and cell proliferation.<sup>48-52</sup> Hence, HSPG/syndecan-1 might also play a role in downstream Wnt signaling in MM. To explore this possibility, *EXT1* ko HMCLs were treated with CHIR9902, which activates Wnt signaling by stabilizing  $\beta$ -catenin. As is shown in Fig.6A, CHIR9902 induced similar levels of Wnt activation in *EXT1* ko cells and empty vector control cells in both XG1 and LME1. In addition, we assessed activation of Wnt-signaling at the receptor level, by measuring phosphorylation of the Wnt co-receptor LRP6. As shown in Fig.6B, simultaneous stimulation with R-spondin and Wnt3a resulted in phosphorylation of LRP6 in both XG1 and LME1, which was clearly inhibited in *EXT1* ko cells. These data indicate that loss of HS interferes with upstream, receptor proximal, Wnt-signaling activation and that HSPGs most likely controls Wnt signaling activity extracellularly, at the level of ligand/receptor interaction.

### **Loss of HS attenuates cell-surface binding of Wnt3a and R-spondin.**

For several growth factors, binding to cell surface HSPGs has been shown to potentiate or to be even essential for signaling.<sup>53,54</sup> For Wnts, binding to HSPGs has been shown in several cell

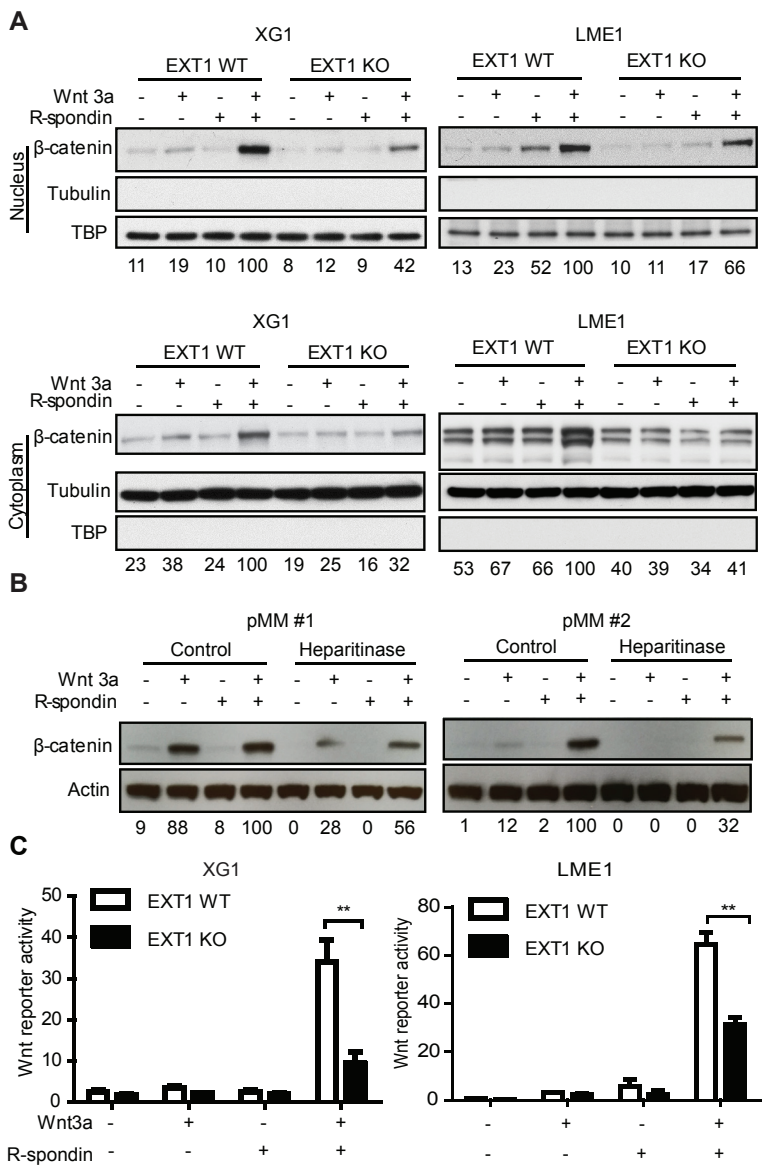


**Figure 5. Loss of HS mitigates the potentiating effect of R-spondin on Wnt signaling.** (A) Western blot analysis of nuclear and cytoplasmic distribution of  $\beta$ -catenin in control transduced (EXT1 WT) or EXT1 KO HMCLs after treatment with recombinant Wnt3a, R-spondin or both. Tubulin (cytoplasm) and TBP (nucleus) served as a fractionation and loading controls. For quantification, the expression level in Wnt3a and R-spondin treated WT cells was normalized to an arbitrary level of 100 units. (B) Western blot analysis of  $\beta$ -catenin accumulation in control (buffer) or heparitinase treated primary MM cells stimulated with recombinant Wnt3a, R-spondin or both. Actin served as a loading control. For quantification, the signal in Wnt3a and R-spondin treated control cells was normalized to an arbitrary level of 100 units. (C) Flow cytometry analysis of Wnt reporter activity in control transduced (EXT1 WT) or EXT1 KO HMCLs treated with Wnt3a, R-spondin or both. Wnt reporter activity is plotted as the percentage of mCherry/TOP.GFP double positive live cells. The mean  $\pm$ SD of 3 independent experiments in triplicate is shown. \*\*,  $P \leq 0.01$  using one-way ANOVA with Bonferroni correction.

types, including *Drosophila* cells and mouse intestinal epithelial cells.<sup>55,56</sup> To study whether HS on MM cells indeed binds Wnt proteins, we employed a flag-tagged,<sup>57</sup> functional Wnt3a protein (Fig.S8) and assessed its binding to the cell surface of *EXT1* ko or empty vector control MM cells. As shown in Fig.7A and Fig.7B, loss of HS resulted in reduced Wnt3a cell surface binding to the HMCL LME1 and primary MM cells.

Like Wnts, R-spondins can also interact with HSPGs. In *Xenopus* embryos, R-spondin-3 binding to syndecan-4 has been shown to mediate Wnt/PCP signaling.<sup>58</sup> To study whether HS moieties on MM cells also bind R-spondin, we employed a His-tagged R-spondin and assessed its binding to the cell surface by flow cytometry. As shown in Fig.7C and Fig.7D, loss of HS completely disrupted the cell surface binding of R-spondin to the HMCL LME1 and primary MM cells. By contrast, ko of *LGR4* (Fig.S9), the cognate R-spondin receptor on MM cells,<sup>34</sup> had no measurable effect on R-spondin cell surface binding (Fig.7C).

All four R-spondins have a common thrombospondin protein (TSP) domain, which mediates glycosaminoglycan (GAG) binding.<sup>59-61</sup> To further study the functional role of R-spondin interaction with HS, we employed a mutant R-spondin (R-spondin- $\Delta$ TSP), which lacks the TSP-domain and C-terminal basic amino-acid-rich domain. As a control, we used R-spondin which lacks the basic amino-acid-rich domain only (R-spondin- $\Delta$ AA). Deletion

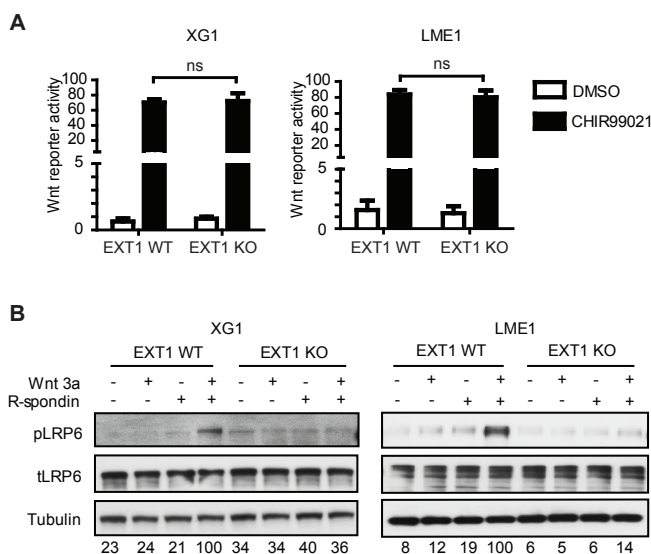


**Figure 6. Loss of HS interferes with upstream, receptor proximal, Wnt pathway activation.** (A) Flow cytometry analysis of Wnt reporter activity in control transduced (EXT1 WT) or EXT1 KO HMCLs XG1 and LME1 treated with the GSK3 inhibitor CHIR99021 or DMSO. Wnt activity is plotted as the percentage of mCherry/TOP.GFP double positive live cells. The mean  $\pm$ SD of 3 independent experiments in triplicate is shown. ns,  $P > 0.05$  using one-way ANOVA with Bonferroni correction. (B) Western blot analysis of phospho-LRP6 (pLRP6) and total LRP6 (tLRP6) in control transduced (EXT1 WT) or EXT1 KO HMCLs XG1 and LME1 treated with Wnt3a, R-spondin or both. Tubulin served as a loading control. For quantification, the phosphorylation level in Wnt3a and R-spondin treated WT cells was normalized to an arbitrary level of 100 units.

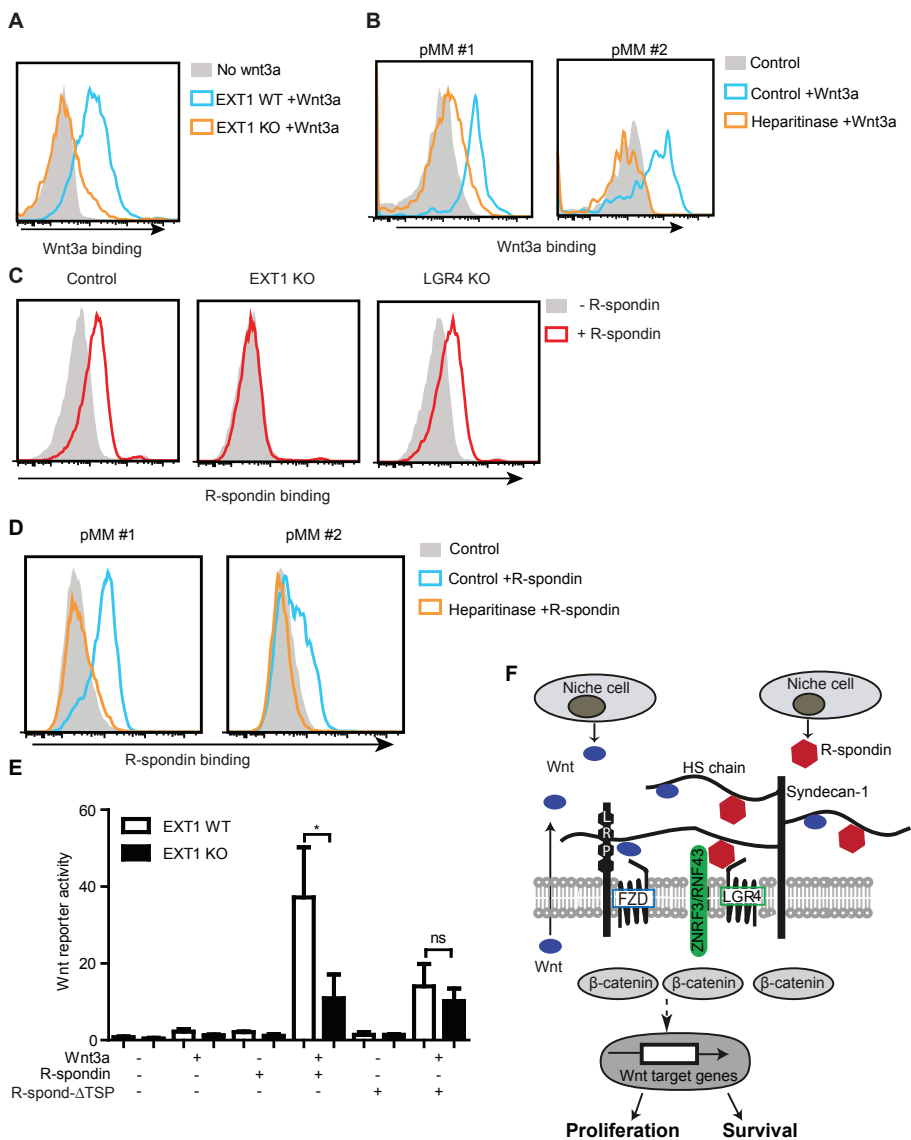


**Figure 7. Loss of HS attenuates cell surface binding of Wnt3a and R-spondin.** (A) Flow cytometry analysis of cell surface binding of Wnt3a-flag on control transduced (EXT1 WT) or EXT1 KO LME1 cells. (B) Flow cytometry analysis of cell surface binding of Wnt3a-flag to primary MM cells treated with heparitinase or buffer (control). (C) Flow cytometry analysis of cell surface binding of R-spondin-his to control empty vector transduced (Control), EXT1 KO and LGR4 KO LME1 cells. (D) Flow cytometry analysis of cell surface binding of R-spondin-his on primary MM cells treated with heparitinase or buffer (control). (E) Flow cytometry analysis of Wnt reporter activity in control transduced (EXT1 WT) or EXT1 KO HMCL treated with Wnt3a, R-spondin-ΔAA or R-spondin-ΔTSP condition medium or their combination. The mean ±SD of 3 independent experiments in triplicate is shown. ns, P > 0.05; \*, P ≤ 0.05 using one-way ANOVA with Bonferroni correction. (F) Model for Syndecan-1 promotes Wnt signaling in MM. In human BM microenvironment, the stromal cells (niche cells) and MM cells secrete Wnt ligands, whereas (pre)osteoblasts (niche cells) produce R-spondins. HS chains decorating syndecan-1 promote autocrine and paracrine Wnt signaling and Wnt-mediated proliferation and survival in MM cells by presenting Wnt ligands and R-spondins.

of the TSP-domain strongly diminished the Wnt-signaling potentiating effect of R-spondin compared to the control R-spondin- $\Delta$ AA. Whereas loss of cell surface HS significantly attenuated the potentiating effect of R-spondin- $\Delta$ AA, it did not affect the (minor) potentiating effect of R-spondin- $\Delta$ TSP on Wnt signaling (Fig.7E). This indicates that the Wnt-signaling promoting effect of R-spondin is largely HS dependent.

Taken together, our data suggests that loss of HS inhibits Wnt signaling by impairing the binding of Wnt ligands and R-spondins to the cell surface.

## Discussion

Aberrant Wnt/ $\beta$ -catenin pathway activity mediates cell proliferation in MM.<sup>18-22,34</sup> In the current study, we reveal that the HS chains decorating syndecan-1 promote autocrine and paracrine Wnt signaling and Wnt-mediated proliferation in MM cells by binding Wnt ligands as well as R-spondins (Fig.7F). These results establish an important role for syndecan-1 in aberrant Wnt/ $\beta$ -catenin signaling and Wnt-ligand mediated cell growth in MM.

We confirm that HMCLs display constitutive Wnt signaling and demonstrate that inhibition of Wnt signaling, either downstream by dnTCF4 or upstream by the Wnt-secretion inhibitors IWP-2 and LGK974, attenuates MM cell growth. These results indicate a role for autocrine Wnt ligands in mediating MM growth. Interestingly, HS-deficient *EXT1* ko HMCLs exhibited decreased levels of cytoplasmic and nuclear  $\beta$ -catenin and a strongly reduced Wnt-reporter activity. Furthermore, in line with a previous study from our laboratory,<sup>6</sup> targeting of HS expression by inducible shRNA-mediated *EXT1* kd resulted in reduced MM cell growth. Interestingly, this growth reduction could largely be reversed by downstream activation of Wnt signaling by means of an active mutant  $\beta$ -catenin (S33Y) or by overexpression of the Wnt-target gene *c-Myc*, suggesting that the attenuated growth may largely be caused by inhibition of Wnt signaling, involving *c-Myc* downregulation.

Although the Wnt pathway is constitutively active in many MMs and HMCLs, these cells still respond to exogenous Wnt ligands.<sup>19,34</sup> In the BM microenvironment these ligands, including Wnt3a, Wnt5a, Wnt10b, and/or Wnt16 are secreted by stromal cells.<sup>19,22,44,45</sup> We employed recombinant Wnt3a, either alone or in combination with R-spondin, to mimic this paracrine stimulation. Importantly, loss of HS significantly reduced the response of MM cells to Wnt3a stimulation and impaired binding of Wnt3a to the MM cell surface. At limiting concentrations of Wnt3a ligand, which presumably represent physiological conditions, the inhibition of Wnt signaling activation caused by *EXT1* ko was much more prominent than at saturating ligand concentrations (Fig.S10). Consistent with these findings, studies in model organisms including *Drosophila* and *Xenopus* have demonstrated that HSPGs are required to increase the local concentration of Wg (Wnt) ligand to activate its receptors.<sup>62,63</sup>

Wnt proteins are relatively unstable and insoluble due to their hydrophobic nature, which constrains long-range signaling.<sup>23</sup> Binding to HSPGs may stabilize Wnt proteins and facilitate their interaction with FZD receptor. In *Drosophila*, abrogation of HS synthesis by mutation of *EXT*-family genes leads to reduced extracellular Wingless levels.<sup>64</sup> Furthermore, in mouse intestinal epithelium, HSPGs were shown to increase the cell surface binding affinity of Wnt ligands, enhancing Wnt/ $\beta$ -catenin signaling, and facilitate crypt regeneration after intestinal epithelial injury,<sup>55</sup> and Alexander et al.<sup>17</sup> reported that syndecan-1 is required for Wnt-mediated mammary tumorigenesis.

R-spondin family proteins have recently been identified as important positive regulators of Wnt signaling by interacting with LGR4-6 receptors.<sup>29,30</sup> In *Xenopus* embryos, R-spondin-3 binds syndecan-4 and mediates Wnt/PCP signaling.<sup>58</sup> Interestingly, we recently found that LGR4 is aberrantly expressed by most MMs, resulting in paracrine Wnt-pathway (hyper)activation by osteoblast-derived R-spondins.<sup>34</sup> Our current results confirm that R-spondin indeed strongly amplifies the response of MM cells to Wnt3a stimulation, and we show that ko of *EXT1*, with consequent loss of HS, disrupts R-spondin binding to the surface of MM cells. Functionally, *EXT1* ko attenuated the capacity of R-spondins to promote Wnt-signaling. All four R-spondins contain a TSP-domain that can bind to HSPGs/heparin.<sup>60,61,65</sup> Deletion of the TSP-domain of R-spondin resulted in a reduced capacity to promote Wnt signaling in MM. Activation of Wnt signaling by this TSP-domain-deficient R-spondin mutant was markedly reduced and was no longer dependent on cell surface HS expression. Together, these data indicate that R-spondins interact with MM cell-surface HS via their TSP-domain. A crystallographic study of the structure of R-spondin1–LGR5–RNF43 showed that the Furin1 domain of R-spondin binds to RNF43 while the Furin 2 domain of R-spondin interacts with LGR5. Hence, the TSP-domain would indeed be accessible for binding other molecules, including HSPGs.<sup>66</sup> Similarly, Glinka et al. also showed that the TSP-domain of the R-spondin is not involved in binding to the LGR receptors.<sup>67</sup> Taken together, these findings suggest that R-spondins potentiate Wnt signaling by interacting with both LGR-receptors and HSPG, interactions that involve distinct R-spondin domains.

Although we found that downstream activation of Wnt signaling by S33Y  $\beta$ -catenin can largely overcome the growth reduction as a consequence of HS deletion, this does by no means exclude a role of HS in mediating other growth factor pathways. For several growth factors, including HGF, EGF-family ligands, and APRIL, interaction with HS has been shown to promote signaling.<sup>5,8</sup> In fact, we have previously found that syndecan-1 HS is even more critical for the MM growth *in vivo* than *in vitro*.<sup>6</sup> In primary MM, distinct MM (sub)clones may differ in their dependence on various HS-binding growth factors for their growth and survival. By targeting HS or its biosynthesis machinery *in vivo*, these will in principle be simultaneously inhibited, thus rendering HS-directed therapy an attractive option. Interestingly, it has recently been shown that a monoclonal antibody primarily

targeting the HS-chains of Glypican-3 inhibited Wnt/ $\beta$ -catenin signaling in hepatocellular carcinoma cells and had potent antitumor activity *in vivo*.<sup>68</sup> However, since HSPGs are widely expressed in normal tissues, generic targeting of HSPGs might cause side effects. These may potentially be circumvented by selective targeting of specific HSPG-modifying enzymes with small molecules or of specific HS-modifications with antibodies or glycomimetics. Indeed, several studies have demonstrated that post-polymerization modifications of HS, such as O-sulfation and epimerization, can specifically modulate the interaction of HSPGs with growth factors, including Wnts.<sup>56,69</sup> Furthermore, as recently shown by Kumagai et.al., the HS-specific endosulfatase-2 can also modulate Wnt signaling in renal cell carcinomas<sup>70</sup>.

Taken together, our results indicate an important role for the syndecan-1 in mediating Wnt/ $\beta$ -catenin signaling and cell growth in MM. Therapeutic targeting of the HS chains decorating syndecan-1 or of the HS biosynthesis and modification machinery may significantly diminish the Wnt/ $\beta$ -catenin signaling-mediated growth of the MMs and may, in addition, also interfere with other growth factor signals emanating from the BM microenvironment.

## Acknowledgments

This work is supported by grant UVA 2011-5205 from the Dutch Cancer Society to M.S. and S.T.P and a CSC Chinese Government Scholarship to Z.R.

## Authorship Contributions

Z.R. designed the research, performed experiments, analyzed the data, designed the figures and wrote the paper; H.v.A, W. d. L, and R. B. H performed experiments. W. d. L., M. M. M., H.C., and M.J.K provided materials. M.S. and S.T.P. supervised the study, designed the research and analyzed the data. S.T.P wrote the paper.

## Conflict of interest

The authors declare no conflict of interest.

## Reference list

1. Lohr JG, Stojanov P, Carter SL, et al. Widespread genetic heterogeneity in multiple myeloma: implications for targeted therapy. *Cancer Cell*. 2014;25(1):91-101.
2. Morgan GJ, Walker BA, Davies FE. The genetic architecture of multiple myeloma. *Nat Rev Cancer*. 2012;12(5):335-348.
3. Lawasut P, Groen RW, Dhimolea E, Richardson PG, Anderson KC, Mitsiades CS. Decoding the pathophysiology and the genetics of multiple myeloma to identify new therapeutic targets. *Semin Oncol*. 2013;40(5):537-548.
4. Hideshima T, Mitsiades C, Tonon G, Richardson PG, Anderson KC. Understanding multiple myeloma pathogenesis in the bone marrow to identify new therapeutic targets. *Nat Rev Cancer*. 2007;7(8):585-598.
5. Derksen PW, Keehnen RM, Evers LM, van Oers MH, Spaargaren M, Pals ST. Cell surface proteoglycan syndecan-1 mediates hepatocyte growth factor binding and promotes Met signaling in multiple myeloma. *Blood*. 2002;99(4):1405-1410.
6. Reijmers RM, Groen RW, Rozemuller H, et al. Targeting EXT1 reveals a crucial role for heparan sulfate in the growth of multiple myeloma. *Blood*. 2010;115(3):601-604.
7. Wijdenes J, Vooijs WC, Clement C, et al. A plasmocyte selective monoclonal antibody (B-B4) recognizes syndecan-1. *Br J Haematol*. 1996;94(2):318-323.
8. Mahtouk K, Cremer FW, Reme T, et al. Heparan sulphate proteoglycans are essential for the myeloma cell growth activity of EGF-family ligands in multiple myeloma. *Oncogene*. 2006;25(54):7180-7191.
9. Yang Y, MacLeod V, Dai Y, et al. The syndecan-1 heparan sulfate proteoglycan is a viable target for myeloma therapy. *Blood*. 2007;110(6):2041-2048.
10. Esko JD, Selleck SB. Order out of chaos: assembly of ligand binding sites in heparan sulfate. *Annu Rev Biochem*. 2002;71:435-471.
11. Lindahl U, Li JP. Interactions between heparan sulfate and proteins-design and functional implications. *Int Rev Cell Mol Biol*. 2009;276:105-159.
12. Hayashi Y, Kobayashi S, Nakato H. Drosophila glypicans regulate the germline stem cell niche. *J Cell Biol*. 2009;187(4):473-480.
13. Bishop JR, Schuksz M, Esko JD. Heparan sulphate proteoglycans fine-tune mammalian physiology. *Nature*. 2007;446(7139):1030-1037.
14. Han C, Belenkaya TY, Khodoun M, Tauchi M, Lin X, Lin X. Distinct and collaborative roles of Drosophila EXT family proteins in morphogen signalling and gradient formation. *Development*. 2004;131(7):1563-1575.
15. Ruoslahti E, Yamaguchi Y. Proteoglycans as modulators of growth factor activities. *Cell*. 1991;64(5):867-869.
16. Reijmers RM, Groen RW, Kuil A, et al. Disruption of heparan sulfate proteoglycan conformation perturbs B-cell maturation and APRIL-mediated plasma cell survival. *Blood*. 2011;117(23):6162-6171.

17. Alexander CM, Reichsman F, Hinkes MT, et al. Syndecan-1 is required for Wnt-1-induced mammary tumorigenesis in mice. *Nat Genet.* 2000;25(3):329-332.
18. Ashihara E, Kawata E, Nakagawa Y, et al. beta-catenin small interfering RNA successfully suppressed progression of multiple myeloma in a mouse model. *Clin Cancer Res.* 2009;15(8):2731-2738.
19. Derksen PW, Tjin E, Meijer HP, et al. Illegitimate WNT signaling promotes proliferation of multiple myeloma cells. *Proc Natl Acad Sci U S A.* 2004;101(16):6122-6127.
20. Dutta-Simmons J, Zhang Y, Gorgun G, et al. Aurora kinase A is a target of Wnt/beta-catenin involved in multiple myeloma disease progression. *Blood.* 2009;114(13):2699-2708.
21. Kocemba KA, Groen RW, van Andel H, et al. Transcriptional silencing of the Wnt-antagonist DKK1 by promoter methylation is associated with enhanced Wnt signaling in advanced multiple myeloma. *PLoS One.* 2012;7(2):e30359.
22. Sukhdeo K, Mani M, Zhang Y, et al. Targeting the beta-catenin/TCF transcriptional complex in the treatment of multiple myeloma. *Proc Natl Acad Sci U S A.* 2007;104(18):7516-7521.
23. Clevers H, Loh KM, Nusse R. Stem cell signaling. An integral program for tissue renewal and regeneration: Wnt signaling and stem cell control. *Science.* 2014;346(6205):1248012.
24. Behrens J, von Kries JP, Kuhl M, et al. Functional interaction of beta-catenin with the transcription factor LEF-1. *Nature.* 1996;382(6592):638-642.
25. Molenaar M, van de Wetering M, Oosterwegel M, et al. XTcf-3 transcription factor mediates beta-catenin-induced axis formation in *Xenopus* embryos. *Cell.* 1996;86(3):391-399.
26. He TC, Sparks AB, Rago C, et al. Identification of c-MYC as a target of the APC pathway. *Science.* 1998;281(5382):1509-1512.
27. Tetsu O, McCormick F. Beta-catenin regulates expression of cyclin D1 in colon carcinoma cells. *Nature.* 1999;398(6726):422-426.
28. Tagde A, Rajabi H, Bouillez A, et al. MUC1-C drives MYC in multiple myeloma. *Blood.* 2016;127(21):2587-2597.
29. de Lau W, Barker N, Low TY, et al. Lgr5 homologues associate with Wnt receptors and mediate R-spondin signalling. *Nature.* 2011;476(7360):293-297.
30. Carmon KS, Gong X, Lin Q, Thomas A, Liu Q. R-spondins function as ligands of the orphan receptors LGR4 and LGR5 to regulate Wnt/beta-catenin signaling. *Proc Natl Acad Sci U S A.* 2011;108(28):11452-11457.
31. Hao HX, Xie Y, Zhang Y, et al. ZNRF3 promotes Wnt receptor turnover in an R-spondin-sensitive manner. *Nature.* 2012;485(7397):195-200.
32. Clevers H, Nusse R. Wnt/beta-catenin signaling and disease. *Cell.* 2012;149(6):1192-1205.
33. Chim CS, Pang R, Fung TK, Choi CL, Liang R. Epigenetic dysregulation of Wnt signaling pathway in multiple myeloma. *Leukemia.* 2007;21(12):2527-2536.
34. van Andel H, Ren Z, Koopmans I, et al. Aberrantly expressed LGR4 empowers Wnt signaling in multiple myeloma by hijacking osteoblast-derived R-spondins. *Proc Natl Acad Sci U S A.* 2017;114(2):376-381.

35. Mani M, Carrasco DE, Zhang Y, et al. BCL9 promotes tumor progression by conferring enhanced proliferative, metastatic, and angiogenic properties to cancer cells. *Cancer Res.* 2009;69(19):7577-7586.
36. Zhao JJ, Lin J, Zhu D, et al. miR-30-5p functions as a tumor suppressor and novel therapeutic tool by targeting the oncogenic Wnt/beta-catenin/BCL9 pathway. *Cancer Res.* 2014;74(6):1801-1813.
37. van Andel H, Kocemba KA, de Haan-Kramer A, et al. Loss of CYLD expression unleashes Wnt signaling in multiple myeloma and is associated with aggressive disease. *Oncogene.* 2016.
38. Sanjana NE, Shalem O, Zhang F. Improved vectors and genome-wide libraries for CRISPR screening. *Nat Methods.* 2014;11(8):783-784.
39. Horst D, Chen J, Morikawa T, Ogino S, Kirchner T, Shivdasani RA. Differential WNT activity in colorectal cancer confers limited tumorigenic potential and is regulated by MAPK signaling. *Cancer Res.* 2012;72(6):1547-1556.
40. Chen B, Dodge ME, Tang W, et al. Small molecule-mediated disruption of Wnt-dependent signaling in tissue regeneration and cancer. *Nat Chem Biol.* 2009;5(2):100-107.
41. Liu J, Pan S, Hsieh MH, et al. Targeting Wnt-driven cancer through the inhibition of Porcupine by LGK974. *Proc Natl Acad Sci U S A.* 2013;110(50):20224-20229.
42. de Alboran IM, O'Hagan RC, Gartner F, et al. Analysis of C-MYC function in normal cells via conditional gene-targeted mutation. *Immunity.* 2001;14(1):45-55.
43. Delmore JE, Issa GC, Lemieux ME, et al. BET bromodomain inhibition as a therapeutic strategy to target c-Myc. *Cell.* 2011;146(6):904-917.
44. McWhirter JR, Neuteboom ST, Wancewicz EV, Monia BP, Downing JR, Murre C. Oncogenic homeodomain transcription factor E2A-Pbx1 activates a novel WNT gene in pre-B acute lymphoblastoid leukemia. *Proc Natl Acad Sci U S A.* 1999;96(20):11464-11469.
45. Van Den Berg DJ, Sharma AK, Bruno E, Hoffman R. Role of members of the Wnt gene family in human hematopoiesis. *Blood.* 1998;92(9):3189-3202.
46. Davidson G, Shen J, Huang YL, et al. Cell cycle control of wnt receptor activation. *Dev Cell.* 2009;17(6):788-799.
47. Acebron SP, Karaulanov E, Berger BS, Huang YL, Niehrs C. Mitotic wnt signaling promotes protein stabilization and regulates cell size. *Mol Cell.* 2014;54(4):663-674.
48. Busch SJ, Martin GA, Barnhart RL, Mano M, Cardin AD, Jackson RL. Trans-repressor activity of nuclear glycosaminoglycans on Fos and Jun/AP-1 oncoprotein-mediated transcription. *J Cell Biol.* 1992;116(1):31-42.
49. Cheng F, Fransson LA, Mani K. Rapid nuclear transit and impaired degradation of amyloid beta and glypican-1-derived heparan sulfate in Tg2576 mouse fibroblasts. *Glycobiology.* 2015;25(5):548-556.
50. Fedarko NS, Ishihara M, Conrad HE. Control of cell division in hepatoma cells by exogenous heparan sulfate proteoglycan. *J Cell Physiol.* 1989;139(2):287-294.
51. Stewart MD, Ramani VC, Sanderson RD. Shed syndecan-1 translocates to the nucleus of cells delivering growth factors and inhibiting histone acetylation: a novel mechanism of tumor-host cross-talk. *J Biol Chem.* 2015;290(2):941-949.

52. Stewart MD, Sanderson RD. Heparan sulfate in the nucleus and its control of cellular functions. *Matrix Biol.* 2014;35:56-59.
53. Paria BC, Elenius K, Klagsbrun M, Dey SK. Heparin-binding EGF-like growth factor interacts with mouse blastocysts independently of ErbB1: a possible role for heparan sulfate proteoglycans and ErbB4 in blastocyst implantation. *Development.* 1999;126(9):1997-2005.
54. Sakaguchi K, Yanagishita M, Takeuchi Y, Aurbach GD. Identification of heparan sulfate proteoglycan as a high affinity receptor for acidic fibroblast growth factor (aFGF) in a parathyroid cell line. *J Biol Chem.* 1991;266(11):7270-7278.
55. Yamamoto S, Nakase H, Matsuura M, et al. Heparan sulfate on intestinal epithelial cells plays a critical role in intestinal crypt homeostasis via Wnt/beta-catenin signaling. *Am J Physiol Gastrointest Liver Physiol.* 2013;305(3):G241-249.
56. Reichsman F, Smith L, Cumberledge S. Glycosaminoglycans can modulate extracellular localization of the wingless protein and promote signal transduction. *J Cell Biol.* 1996;135(3):819-827.
57. Farin HF, Jordens I, Mosa MH, et al. Visualization of a short-range Wnt gradient in the intestinal stem-cell niche. *Nature.* 2016;530(7590):340-343.
58. Ohkawara B, Glinka A, Niehrs C. Rspo3 binds syndecan 4 and induces Wnt/PCP signaling via clathrin-mediated endocytosis to promote morphogenesis. *Dev Cell.* 2011;20(3):303-314.
59. Ayadi L. Molecular modelling of the TSR domain of R-spondin 4. *Bioinformatics.* 2008;3(3):119-123.
60. Tan K, Duquette M, Liu JH, et al. Crystal structure of the TSP-1 type 1 repeats: a novel layered fold and its biological implication. *J Cell Biol.* 2002;159(2):373-382.
61. Chang CF, Hsu LS, Weng CY, et al. N-Glycosylation of Human R-Spondin 1 Is Required for Efficient Secretion and Stability but Not for Its Heparin Binding Ability. *Int J Mol Sci.* 2016;17(6).
62. Baeg GH, Lin X, Khare N, Baumgartner S, Perrimon N. Heparan sulfate proteoglycans are critical for the organization of the extracellular distribution of Wingless. *Development.* 2001;128(1):87-94.
63. Itoh K, Sokol SY. Heparan sulfate proteoglycans are required for mesoderm formation in *Xenopus* embryos. *Development.* 1994;120(9):2703-2711.
64. Bornemann DJ, Duncan JE, Staatz W, Selleck S, Warrior R. Abrogation of heparan sulfate synthesis in *Drosophila* disrupts the Wingless, Hedgehog and Decapentaplegic signaling pathways. *Development.* 2004;131(9):1927-1938.
65. Nam JS, Turcotte TJ, Smith PF, Choi S, Yoon JK. Mouse cristin/R-spondin family proteins are novel ligands for the Frizzled 8 and LRP6 receptors and activate beta-catenin-dependent gene expression. *J Biol Chem.* 2006;281(19):13247-13257.
66. Chen PH, Chen X, Lin Z, Fang D, He X. The structural basis of R-spondin recognition by LGR5 and RNF43. *Genes Dev.* 2013;27(12):1345-1350.
67. Glinka A, Dolde C, Kirsch N, et al. LGR4 and LGR5 are R-spondin receptors mediating Wnt/beta-catenin and Wnt/PCP signalling. *EMBO Rep.* 2011;12(10):1055-1061.

## CHAPTER 3

68. Gao W, Kim H, Feng M, et al. Inactivation of Wnt signaling by a human antibody that recognizes the heparan sulfate chains of glypican-3 for liver cancer therapy. *Hepatology*. 2014;60(2):576-587.
69. Hacker U, Nybakken K, Perrimon N. Heparan sulphate proteoglycans: the sweet side of development. *Nat Rev Mol Cell Biol*. 2005;6(7):530-541.
70. Kumagai S, Ishibashi K, Kataoka M, et al. The impact of Sulfatase-2 on cancer progression and prognosis in patients with renal cell carcinoma. *Cancer Sci*. 2016.

## Supplemental Methods

### Flow cytometry

For heparan sulfate staining, cells were incubated with 10E4 antibody (Amsbio) or isotype control IgM (DAKO) followed by staining with anti-mouse IgM-APC (Southern Biotech). For the Wnt3a cell surface binding, cells were incubated with 200ul Wnt3a-flag conditioned medium at 4°C for 90 minutes. After washing three times, cells were stained with anti-flag M2 antibody (Sigma Aldrich). Primary antibodies were detected with rabbit anti-mouse IgG1-APC (Southern Biotech). For the R-spondin cell surface binding, cells were incubated with 200ul R-spondin-His conditioned medium at 4°C for 90 minutes. After washing three times, cells were stained with rabbit anti-His antibody (Abcam). Primary antibodies were detected with swine anti-rabbit-FITC (DAKO). The staining was analyzed by flow cytometry. For LGR4 staining, cells were incubated with hybridoma supernatant containing hLGR4 specific rat monoclonal IgG2b antibody,<sup>101</sup> followed by staining with biotinylated mouse-anti-rat IgG2b (Biolegend) and streptavidin-APC (Southern Biotech).

### Confocal microscopy

The reduction in heparan sulphate expression after *EXT-1* knock-out was evaluated by confocal microscopy. Cells were fixed with 4% PFA (Hatfield) for 15 minutes at room temperature. Samples were subsequently washed (TBS, 0,5% BSA) and quenched (50 mM NH<sub>4</sub>Cl and 0.5% BSA in TBS) for 15 minutes. After washing, samples were blocked for 30 minutes in TBS, 0.5% BSA with human Fc-block (Miltenyi Biotech) and stained with HSPG antibody 10E4 (1:500) (US Biological). After washing, cells were stained with directly Alexa Fluor 488 conjugated goat anti-mouse IgM (Thermo Scientific). Then cells were mounted using MOWIOL (Calbiochem, EMD Millipore) supplemented with 2.5% triethylenediamine (Sigma-Aldrich) and 1 µg/mL Hoechst 33342 (Life Technologies,). Samples were imaged using 63x objective on a Leica TCS SP8 confocal microscope and analyzed using Leica Application Suite X (Leica Microsystems).

### In vitro cell growth and apoptosis

For the cell growth assay, cells were plated ( $1 \times 10^4$ ) in 96-well plates and cultured for indicated days. Cells were quantified by flow cytometry, employing 7-AAD (Thermo Fisher Scientific) to exclude dead cells. For shRNA transduced cells, 1µg/ml doxycycline (Sigma Aldrich) is used 4 days before growth assay to induce knock down. For the co-culture assay, BMSC cells HS5 expressing GFP were plated ( $1.5 \times 10^4$ ) one day before adding the MM cells.

For the apoptosis assay,  $1 \times 10^5$  cells were stained with Annexin V FITC (IQ Products) and TO-PRO-3 (Thermo Fisher Scientific), cell apoptosis was analyzed by flow cytometry.

### **Cell cycle analysis**

For cell cycle analysis of Wnt responsive cells, TOP.GFP transduced HMCLs were stimulated with recombinant Wnt3a for 24h, after which GFP- and GFP+ cells were FACS sorted. For phospho histone H3 staining, FACS sorted cells were fixed and stained with the phosphorylated histone H3 phosflow antibody (clone HTA28, BD) using the BD Cytofix/Cytoperm kit and subsequently stained with propidium iodide (Invitrogen technologies).

### **Immunoblotting**

Protein samples were separated by 10% SDS-polyacrylamide gel electrophoresis and subsequently blotted. Nuclear and cytosolic fractions were prepared using the Nuclear/Cytosolic fractionation kit (Biovision) according to the manufacturer's instructions. The antibodies used were:  $\beta$ -tubulin (Sigma Aldrich),  $\beta$ -catenin (BD Biosciences), c-Myc (Epitomics), cyclin D1, ERK, AKT (Santa Cruz), LRP6, Phospho-LRP6, Phospho-ERK, Phospho-AKT (Cell Signaling), and TBP (Abcam). Primary antibodies were detected by HRP-conjugated secondary antibodies (DAKO), followed by detection using Amersham ECL Westernblot Detection Reagent (GE Healthcare). Western blot is quantified by ImageJ.

## Supplemental data

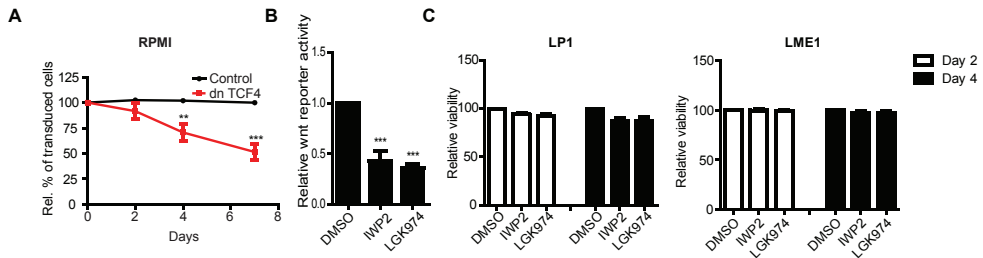


Figure S1. (A) Percentage of transduced cells in RPMI transduced with empty vector control or dn.TCF4 expressed from bicistronic lentiviral vectors, relative to day 0. The mean  $\pm$ SD of 3 independent experiments in triplo is shown. \*\*,  $P \leq 0.01$ ; \*\*\*,  $P \leq 0.001$  using unpaired student's t test. (B) Flow cytometry analysis of the effect of the small molecule Wnt secretion inhibitors IWP-2 (2.5 $\mu$ M) and LGK974 (2.5 $\mu$ M) on the Wnt reporter activity in HMCL LP1. The Wnt reporter activity of non-treated cells was normalized to 1. The mean  $\pm$ SD of 3 independent experiments in triplo is shown. \*\*\*,  $P \leq 0.001$  using one-way ANOVA with Bonferroni correction. (C) Flow cytometry analysis of the effect of the small molecule Wnt secretion inhibitors IWP-2 (2.5 $\mu$ M) and LGK974 (2.5 $\mu$ M) on HMCLs cell viability after 4 days. The mean  $\pm$ SD of 3 independent experiments in triplo is shown.

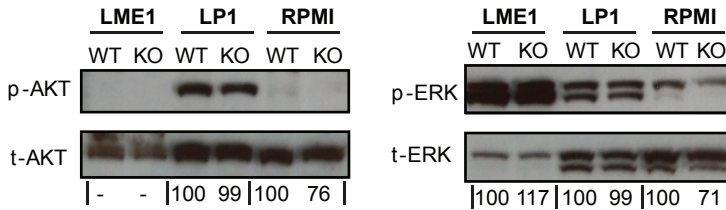


Figure S2. Western blot analysis of phospho-AKT and phospho-ERK in control transduced (WT) or EXT1 KO HMCLs. Total AKT and total ERK served as loading control. For quantification, the expression level in WT cells was normalized to an arbitrary level of 100 units.

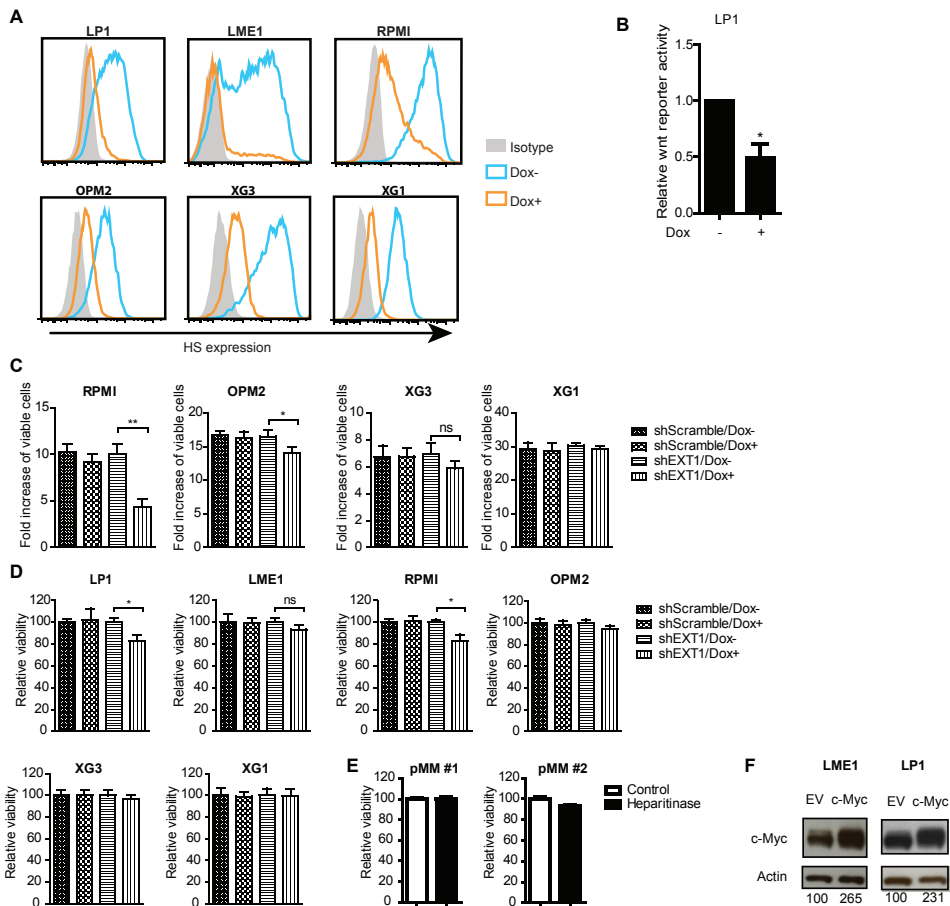


Figure S3. (A) Flow cytometry analysis of cell surface expression of HS in doxycycline (Dox) induced EXT1 knock-down (kd) in HMCLs. Cells were treated with doxycycline (Dox) for 4 days to induce kd. (B) Flow cytometry analysis of Wnt reporter activity in LP1 EXT1 kd cells. Wnt reporter activity is plotted as the percentage of mCherry/GFP double positive live cells. The Wnt reporter activity of non-treated cells was normalized to 1. The mean  $\pm$ SD of 3 independent experiments in triplo is shown. \*,  $P \leq 0.05$  using one sample t-test. (C) Flow cytometry analysis of the effect of doxycycline (Dox)-induced EXT1 kd on HMCL expansion at 5 days of culture, relative to day 0. shScramble is used as control. The mean  $\pm$ SD of 3 independent experiments in triplicate is shown, \*\*,  $P \leq 0.01$  using unpaired student's t test. (D) Flow cytometry analysis of the effect of doxycycline (Dox) induced EXT1 kd on HMCL viability. shScramble is used as control. The % of viable non-treated cells was normalized to 100. The mean  $\pm$ SD of 3 independent experiments in triplicate is shown. ns, not significant; \*,  $P \leq 0.05$  using unpaired student's t test. (E) Flow cytometry analysis of primary MM cell viability after heparitinase or control buffer treatment. (F) Western blot analysis of c-Myc expression in empty vector (EV) control or c-Myc transduced HMCLs. For quantification, the expression level in empty vector (EV) control transduced cells was normalized to an arbitrary level of 100 units.

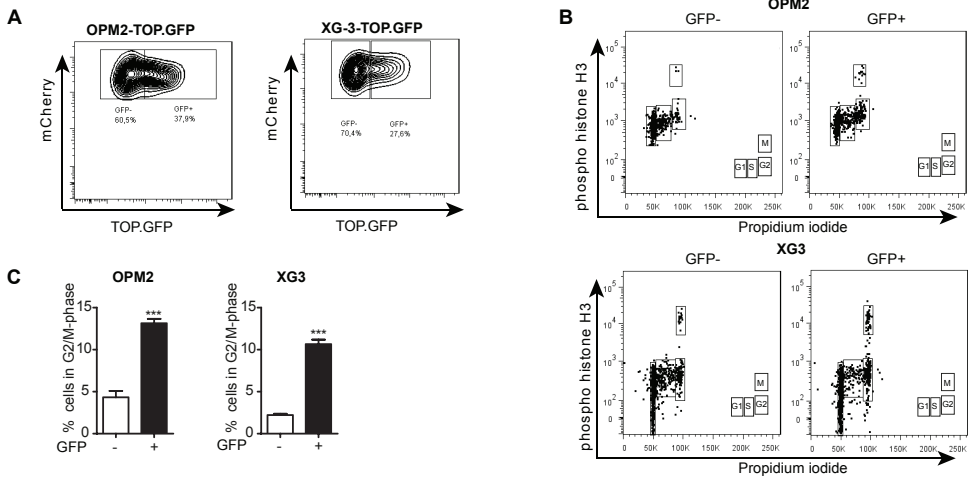


Figure S4. Cell cycle analysis of Wnt responsive cells. (A) TOP.GFP transduced HMCLs were treated with Wnt3a for 24h. Wnt responsive cells were gated as GFP+ and non-responsive cell as GFP-. Cells were sorted by flow cytometry. (B) GFP+ and GFP- sorted cells were stained with anti-phospho-histone H3 and propidium iodide. Representative plots of cell cycle analysis are shown. (C) Quantification of the % of cells in the G2/M-phase in the GFP- and GFP+ subpopulation, The mean  $\pm$ SD of 3 independent experiments in triplo is shown. \*\*\*,  $P \leq 0.001$  using unpaired student's test.

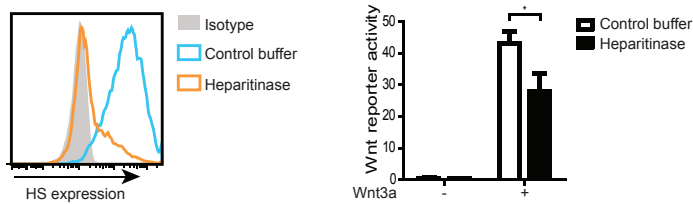


Figure S5. Enzymatic removal of cell-surface HS by means of heparitinase attenuated Wnt/ $\beta$ -catenin signaling in MM. Left panel: OPM2 cells were treated with Heparitinase or HBSS buffer (control) for 2h. Expression of cell surface HS was measured by flow cytometry using 10E4 antibody. Right panel: Flow cytometry analysis of Wnt reporter activity after Heparitinase or control buffer treatment, TOP-GFP transduced OPM2 cells were stimulated with Wnt3a for 24 hour. Wnt reporter activity is plotted as the percentage of mCherry/TOP.GFP double positive cells (right panel). The mean  $\pm$ SD of 3 independent experiments in triplo is shown. \*,  $P \leq 0.05$  using one-way ANOVA with Bonferroni correction.

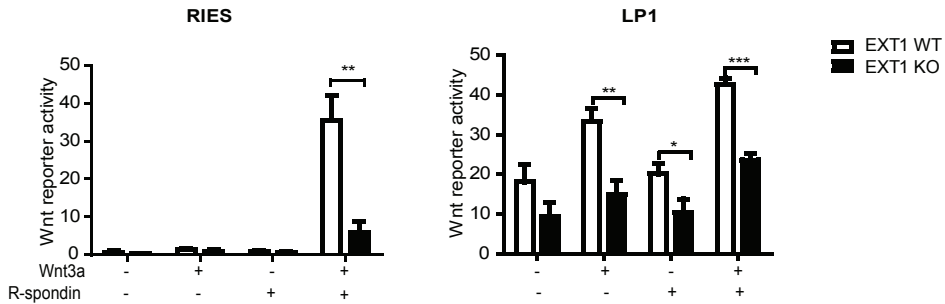


Figure S6. Flow cytometry analysis of Wnt activity in control transduced (EXT1 WT) or EXT1 KO HMCL RIES and LP1 treated with Wnt3a, R-spondin or both. Wnt activity is plotted as the percentage of mCherry/TOP.GFP double positive live cells. The mean  $\pm$ SD of 3 independent experiments in triplo is shown. \*,  $P \leq 0.05$ ; \*\*,  $P \leq 0.01$ ; \*\*\*,  $P \leq 0.001$  using one-way ANOVA with Bonferroni correction.

3

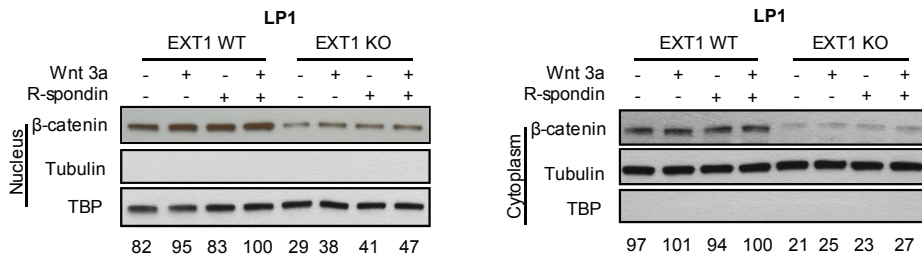


Figure S7. Western blot analysis of nuclear and cytoplasmic distribution of  $\beta$ -catenin in control transduced (EXT1 WT) or EXT1 KO LP1 after treatment with recombinant Wnt3a, R-spondin or both. Tubulin (cytoplasm) and TBP (nucleus) served both as fractionation and loading controls. For quantification, the expression level in Wnt3a and R-spondin treated WT cells was normalized to an arbitrary level of 100 units.

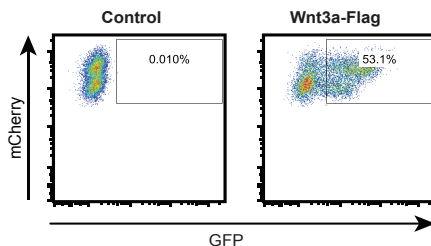


Figure S8. Flag tagged Wnt3a is functionally active. Flow cytometry analysis of Wnt reporter activity on TOP.GFP transduced OPM2 cells stimulated with Wnt3a-flag condition medium for 24 hour.

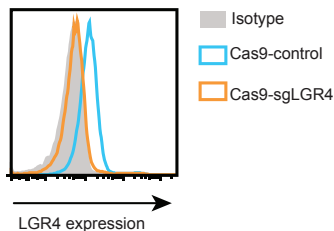


Figure S9. CRISPR induced LGR4 KO. Flow cytometry analysis of cell surface expression of LGR4 in control transduced (Cas9-control) or CRISPR/CAS9 mediated LGR4 KO (Cas9-LGR4) in HMCL LME1 cell

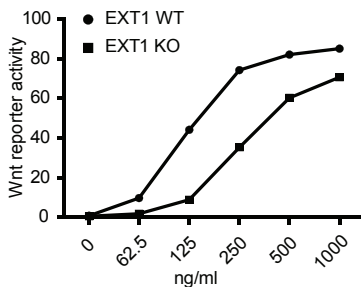


Figure S10. Stimulation of control transduced (EXT1 WT) or EXT1 KO OPM2 TOP-GFP cells with titrated Wnt3a. Wnt reporter activity is plotted as the percentage of mCherry/TOP.GFP double positive cells.